The NCO + NO Reaction Revisited: Ab Initio MO/VRRKM Calculations for Total Rate Constant and Product Branching Ratios

Rongshun Zhu and M. C. Lin*

Department of Chemistry, Emory University, Atlanta, Georgia 30322

Received: July 24, 2000; In Final Form: September 11, 2000

The mechanism for the NCO + NO reaction has been studied using a high-level ab initio molecular orbital G2M method in conjunction with variational RRKM calculations. The results indicate that the reaction occurs primarily via the following singlet potential energy surface: (1) NCO + NO ⇌ OCNNO → N_2O + CO; (2) NCO + NO ⇌ OCNNO → c-OC(O)NN− → N_2 + CO_2. Cis-OCNNO is the main intermediate to form these products. The decomposition of cis-OCNNO to the products N_2O + CO is energetically less favorable than the cyclization process forming c-OC(O)NN− by 8.2 kcal/mol, but both processes take place via tight transition states. These tight transition states coupling with the loose association channel give rise to the experimentally observed strong negative temperature dependence. Calculated results also indicate that the total and individual rate constants have a strong angular-momentum dependence. The calculated values are in good agreement with experimental data both for the rate constant and product branching ratios. These results are qualitatively consistent with those predicted previously by the conventional RRKM calculations based on the energetics computed at the BAC-MP4 level of theory.

1. Introduction

The isocyanate radical, NCO, is a key intermediate in the RAPRENO$_x$ (rapid reduction of nitrogen oxides) process using cyanuric acid to reduce the emission of nitrogen oxides from internal-combustion engines.[1,2] The reaction of NCO with NO is one of the most important reactions in this system, which produces N_2O, CO, and CO_2 via the following three possible channels:

$$\mathrm{NCO + NO \rightarrow N_2O + CO} \quad \text{(a)}$$

$$\rightarrow \mathrm{N_2 + CO_2} \quad \text{(b)}$$

$$\rightarrow \mathrm{N_2 + O + CO} \quad \text{(c)}$$

Several research groups have experimentally measured the total rate constant for the reaction[3−14] and three groups have reported its product branching ratios.[9,12,15] Becker et al.[12] reported that (b) is the major channel, with the branching ratio of a:b = 0.35:0.65 from their FTIR absorption measurement of the stable products. This is in reasonable agreement with the results of Cooper et al.,[9] who obtained the ratio, a:b = 0.44:0.56, for the temperature range 296−623 K from diode laser absorption measurements. The product channel (c) is believed to be negligible according to the experiment of these authors. In contrast, Jones and Wang[15] have reported that the N_2O and CO are the main products; they detected the products with a coherent anti-Stokes Ramam scattering (CARS) technique and observed no N_2 formation. For the total rate constant determination, Perry's study by monitoring the disappearance of NCO indicated that the reaction had a strong negative temperature dependence, but no pressure effect was noted.[3] Similar strong negative temperature dependencies were reported by Juang and co-workers[10] and by Mertens et al. studied in shock waves.[7] Combination of the low-temperature and high-temperature shock-tube data results in a very pronounced negative temperature dependence.

To elucidate the mechanism of this important process, Lin et al.[16] have performed a quantum chemical calculation using the BAC-MP4 method.[17−19] The rate constants for the overall as well as individual channels were calculated by means of the RRKM theory.[20] However, in their calculations the transition state for the association process NCO + NO → OCNNO was not directly computed quantum mechanically and the reproduction of the experimentally observed branching ratio[9,12] from RRKM calculations required a downward adjustment of the transition state energy for channel (a) by 3.6 kcal (15% of the barrier height). In this study, we carried out variational RRKM calculations based on the energies and structures predicted by a high-level molecular orbital method.

2. Computation Methods

2.1. Ab Initio MO Calculations. The geometries of the reactants, intermediates, transition states, and products for the NCO + NO reaction have been optimized at the hybrid density functional B3LYP/6-311G (d, p) level of theory, i.e., Beck's three-parameter nonlocal-exchange functional [21−23] with the nonlocal correlation functional of Lee et al.[24] The vibrational frequencies, calculated at this level have been used for characterization of stationary points, zero-point energy (ZPE) corrections, and RRKM calculations. All the stationary points have been identified for local minima (with the number of imaginary frequencies equal to zero) and transition states (each with one imaginary frequency). Intrinsic reaction coordinate (IRC) calculations[25] have been performed to confirm the connection between transition states and designated intermediates.

* Corresponding author. E-mail: chemmcl@emory.edu.

10.1021/jp002637a CCC: $19.00
Published on Web 10/21/2000

TABLE 1: Total and Relative Energies of Reactants, Intermediates, Transition States, and Products for the Reaction of NCO with NO Calculated at Different Levels of Theory with B3LYP/6-311G Optimized Geometries**

	Energies[b]				
Species	ZPE[a]	B3LYP/6-311G (d, p)	MP2/6-311G(d, p)	MP2/6−311+G(3df, 2p)	CCSD(T)/6-311G (d, p)	G2M
NCO + NO	9.1	−297.97671	−297.23272	−297.4058971	−297.29181	−297.51212
trans-OCNNO C_s, A′	11.6	−37.2	−46.6	−51.1	−32.4	−40.0
TS1, C_s, A′	8.8	32.5	27.5	23.2	27.5	17.1
N_2O + CO	9.4	−51.9	−76.5	−77.5	−57.9	−64.3
cis-OCNNO C_s, A′	11.4	−32.8	−42.5	−47.1	−28.5	−36.5
TS2, C_s, A′	10.6	−7.3	−13.9	−19.2	−5.7	−15.1
TS3, c-OC(=O)NN−	11.4	−12.6	−24.9	−32.4	−12.4	−23.3
c-OC(=O)NN−	11.7	−21.1	−35.4	−42.3	−24.2	−34.3
TS4, C_s, A′	11.1	−21.0	−35.3	−41.8	−23.6	−33.8
N_2 + CO_2	10.8	−138.3	−164.2	−164.7	−145.8	−150.2
trans-OCNNO, C_s, ^{3}A″	11.4	−0.69	6.6	2.9	11.4	7.5
cis-OCNNO, C_s, ^{3}A″	11.3	4.1	10.2	6.6	15.4	11.4

[a] Zero-point energy (kcal/mol), calculated at the B3LYP/6-311G (d, p) level. [b] The total energies for NCO + NO are given in hartree. For other species, relative energies (kcal/mol) with respect to NCO + NO (with ZPE included at the G2M level).

To obtain more reliable energies, the modified G2M(RCC, MP2) method[26] has been used. The total energy in G2M(RCC, MP2) is calculated as follows:[26]

$$E[\text{G2M(RCC, MP2)}] = E[\text{RCCSD(T)/6-311G(d, p)}] + \Delta E(+3\text{df, 2p}) + \Delta E(\text{HLC}) + \text{ZPE[B3LYP/6-311G(d, p)]}$$

Here,

$$\Delta E(+3\text{df, 2p}) = E[\text{MP2/6-311 + G(3df, 2p)}] - E[\text{MP2/6-311G(d, p)}]$$

and

$$\Delta E(\text{HLC}) = -0.00525\ n_\beta - 0.00019\ n_\alpha$$

where HLC represents the small empirical "higher level correction"; n_α and n_β are the numbers of valence electrons, $n_\alpha \geq n_\beta$. All calculations were carried out with Gaussian 98[27] and MOLPRO 96[28] programs.

2.2. VTST Calculations for the Association Step. The association of NCO with NO forming intermediate OCNNO does not have a well-defined transition state because of the absence of reaction barrier; a variational transition state theory (VTST) calculation has to be carried out as described below. The OCNNO intermediate formed in the association reaction has two isomers: cis-OCNNO and trans-OCNNO. The cis-isomer is the main intermediate producing the major products N_2O + CO and N_2 + CO_2. First, we calculated the potential energy surface for the approach of NCO and NO forming cis-OCNNO. The forming N−N bond distance was varied from its equilibrium value 1.543 Å to 3.5 Å with an interval of 0.1 Å. Despite our numerous attempts, we were unable to obtain a reliable PES at the B3LYP/6-311G (d, p) level of theory, the energy curve increases monotonically and cannot be improved by mere energy corrections in the framework of the G2M method. Similar phenomenon was found in other system.[29] Two possible factors contributed to the monotonic increase of energy: One is the larger spin contamination at longer N−N distances (>2.3 Å) because of the spin variation from singlet at shorter N−N bond lengths to almost triplet at longer N−N distances. The other factor is that with the N−N bond lengthening, the distance between the two O atoms decreases; accordingly, the repulsion energy increases, leading to the monotonic increase in total energy. To overcome these problems, we use mixed wave functions and fix the NNO bond angle in the cis-OCNNO configuration at 115.5° and the N−N bond changes from 1.543 Å to 3.5 Å with an interval of 0.1 Å as before. Other geometric parameters were optimized for each N−N separation. For each structure, we calculated the 3N-7 vibrational frequencies, projected out of the gradient direction. In this manner, a smooth and reasonable potential curve was obtained. The B3LYP calculated total energy at each point along the reaction path was used to evaluate the Morse potential energy function and then scaled to match the dissociation energy predicted at the G2M level of theory.

The resulting potential energy function $E(R)$ is given by

$$E(R) = D_e\,[1 - e^{-\beta(R-R_e)}]^2$$

where D_e = 36.09 kcal/mol, β = 1.743 Å^{-1}, and R_e = 1.543 Å is the equilibrium value of R, i.e., the equilibrium N−N bond length in cis-OCNNO as alluded to above. This potential for the association process was used in all subsequent RRKM calculations.

3. Results and Discussion

3.1. The Potential Energy Surface. Because the O atom formation channel (c) is of negligible importance and the triplet states cis-OCNNO and trans-OCNNO have higher energies (see Table 1), we focus our study on the formation of N_2O and CO_2 by channels (a) and (b), respectively, as was done in our previous calculations based on the BAC-MP4 method.[16] The optimized geometries of the reactants, intermediates, transition states, and products are shown in Figure 1; the potential energy diagram obtained at the G2M level is presented in Figure 2; the total and relative energies are compiled in Table 1; and the vibrational frequencies and moment of inertia of all species are summarized in Table 2.

As mentioned above, the OCNNO intermediate formed in the NCO + NO reaction has two isomers, whose energies at the G2M level of theory are 36.5 and 40.0 kcal/mol lower than that of the reactants for the cis- and trans-isomers, respectively. Although the trans-isomer is more stable, about 4 kcal/mol, than its cis-isomer, it cannot yield products competitively. From Figure 2, we can see that the energy of TS1 is about 32.2 kcal/mol higher than that of TS2; it is thus much less efficient to form N_2O + CO directly from trans-OCNNO. On the contrary, cis-OCNNO can efficiently produce N_2O + CO and N_2 + CO_2 via channels (a) and (b). The decomposition of the cis-OCNNO intermediate producing the N_2O + CO products occurs via a simple bond-fission with a very tight transition state (TS2), in which the breaking C−N bond is 0.371 Å longer than that in the cis-intermediate. This process is energetically less favorable

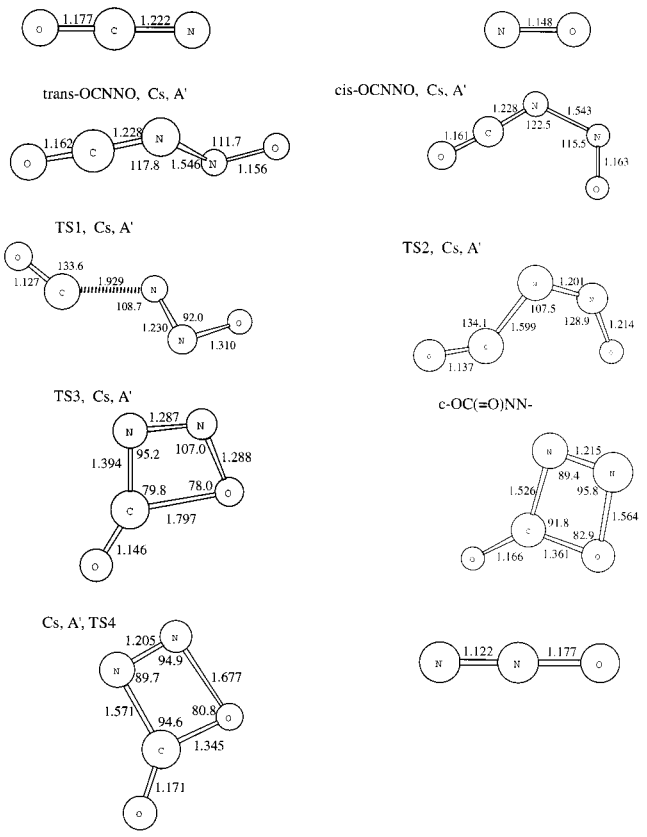

Figure 1. The optimized geometries of the reactants, intermediates, transition states, and products at the B3LYP/6-311G(d, p) level.

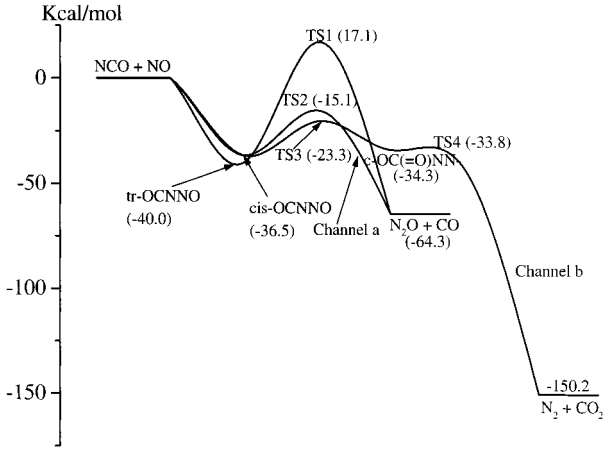

Figure 2. Energy diagram of the NCO−NO system computed at the G2M level.

than the cyclization step. The cis-isomer can form a cyclic intermediate (c-OC(O)NN−) via a very tight four centers transition state (see TS3 in Figure 1) whose energy is 23.3 kcal/mol below the reactants. In TS3, the forming C−O bond, 1.797 Å, is 0.436 Å longer than that in c-OC(═O)NN−. The c-OC(═O)NN− intermediate is about 2 kcal/mol less stable than cis-OCNNO and it can readily decompose to $N_2 + CO_2$ with a barrier of only 0.5 kcal/mol at the G2M level. Overall, both channels are highly exothermic.

3.2. Microcanonical E-Resolved and *E*,*J*-Resolved RRKM Calculations for Total and Individual Rate Constants. In the association process, a statistical treatment of the conserved-mode contribution to the transition-state partition functions was performed variationally;[30−33] the step size of 1.00 cm^{-1} is used for the convolution of the conserved-mode vibrations and the

TABLE 2: Vibrational Frequencies and Moments of Inertia of All Species

Species	I_a, I_b, I_c (amu)	Frequencies (cm^{-1})		
NCO	0	504.7	586.3	1298.8
	153.6	2000.6		
	153.6			
NO	0	1988.44		
	35.2			
	35.2			
N_2O	0	595.7	1368.6	2401.2
	141.3			
	141.3			
CO	0	2219.9		
	31.1			
	31.1			
N_2	0	2447.4		
	30.0			
	30.0			
trans-OCNNO	29.5	117.2	168.4	389.7
	690.9	627.8	654.4	765
	720.4	1332.4	1786.3	2278.6
cis-OCNNO	97.8	99.5	134.7	331.6
	498.3	630.7	699.7	794.3
	596.1	1305.1	1744.2	2260.2
trans-OCNNO → CO + N_2O	32.2	508 i	86	142.2
(TS1)	779.4	319.2	326.1	495.1
	811.7	987.7	1587.9	2195.6
cis-OCNNO → CO + N_2O	91.9	617.7 i	134.7	156.2
(TS2)	495.4	411.7	632.9	869.8
	587.3	1346.7	1728.1	2122.2
cis-OCNNO → c−C(═O)NN−	113	405.7 i	256.1	428.4
TS3	327.9	737.5	753.7	1075.4
	440.9	1226.7	1357.2	2130.2
c-OC(═O)NN−	114.1	168.3	275.3	471.5
	300.1	727.1	773.9	966.1
	415.1	1111.1	1660.2	2012.4
c-OC(═O)NN− → CO_2+N_2	121.2	470.2 i	285.5	454.4
TS4	305.6	698.5	760.1	846
	426.8	1093.3	1671.4	1978.6

step size of 50.00 cm^{-1} was used for the generation of the transitional-mode number of states. The numbers of states are evaluated according to the variable reaction coordinate flexible transition state theory.[30,31] The Morse potential with $\beta = 1.743$ $Å^{-1}$, $D_e = 36.4$ kcal/mol derived above was employed for this process. The component rates were evaluated with the *E*- and *E*,*J*-resolved RRKM calculations. The pressure dependence was treated by 1-D master equation calculations using the Boltzmann probability of the complex for the J distribution. The master equation was solved by an inversion-based approach.[32,33]

The energy-transfer rate coefficients were computed on the basis of the exponential down model with the $\langle\Delta E\rangle$ down value of 400 cm^{-1}. To achieve convergence in the integration over the energy range, an energy grain size of 30 cm^{-1} was used, this grain size provides numerically converged results for all temperature studies with an energy spanning range, from 15000 cm^{-1} below to 24000 cm^{-1} above the threshold. The total angular momentum *J* covered the range from 0 to 246 in steps of 5 for the *E*,*J*-resolved calculation. The Lennard-Jones parameters for OCNNO−Ar pair were assumed to be the same as those of the OCNO−Ar pair, $\sigma = 3.9$ Å and $\epsilon = 205$ K.[33]

In the RRKM calculations, we neglected the effect of TS4 because its energy is about 10 kcal/mol lower than TS2 and the rate-controlling step in this channel is TS2. For TS2 and TS3, the numbers of states were evaluated according to the rigid-rotor harmonic-oscillator assumption. The frequencies and energies used in the RRKM calculations were obtained by the B3LYP/6-311G (d, p) and G2M methods, respectively. All the rate constants and product branching ratio were calculated using the Variflex program.[33]

TABLE 3: Calculated Values of Total and Individual Channel Rate Constants for the NCO + NO Reaction as a Function of Temperature[a]

T/K	$k(E)_t$	$k(E)_a$	$k(E)_b$	$k(E,J)_t$	$K(E,J)_a$	$k(E,J)_b$
300	2.84	1.19	1.64	2.28	0.96	1.32
400	2.26	0.99	1.26	1.81	0.79	1.01
500	1.89	0.87	1.02	1.51	0.70	0.81
600	1.61	0.77	0.84	1.30	0.63	0.68
700	1.40	0.70	0.71	1.14	0.57	0.57
800	1.23	0.63	0.59	1.01	0.53	0.49
1000	0.97	0.53	0.44	0.82	0.45	0.36
1200	0.78	0.45	0.33	0.67	0.39	0.28
1500	0.56	0.34	0.22	0.49	0.30	0.19
1800	0.39	0.24	0.14	0.35	0.22	0.13
2000	0.30	0.19	0.11	0.27	0.17	0.10
2500	0.15	0.10	0.05	0.14	0.09	0.05
3000	0.08	0.05	0.03	0.07	0.05	0.02

[a] Rate constants are calculated at 100 Torr, given in units of 10^{13} cm^3 mol^{-1} s^{-1}.

TABLE 4: Branching Ratio ($k_b/(k_a + k_b)$)[a]

T/K	300	400	500	600	700	800	1000	1200
ratio (*E*)	0.579	0.559	0.540	0.518	0.500	0.482	0.448	0.418
ratio (*E*,*J*)	0.580	0.560	0.540	0.521	0.502	0.485	0.450	0.421

T/K	1500	1800	2000	2500	3000
ratio (*E*)	0.38	0.365	0.356	0.339	0.330
ratio (*E*,*J*)	0.389	0.367	0.357	0.341	0.332

[a] Ratio (*E*) and Ratio (*E*,*J*) represent *E*-resolved and *E*,*J*-resolved branching ratio $k_b/(k_a + k_b)$, respectively.

Table 3 presents the total and individual channel rate constants for the NCO + NO reaction as a function of temperature; the calculated rate constants are plotted in Figure 3 for comparison with experimental values. The results show that for total and individual rate constants, the *E*-resolved rate constants are 10−25% higher than the *E*,*J*-resolved values in the 300−3000 K temperature range (see Table 3). This is similar to the differences observed in other radical reactions: 5−10% for $CH_3 + H \rightarrow CH_4$ (300−2500 K)[34] and 20% for $2\ CH_3 \rightarrow C_2H_6$ (300−2000 K).[35] The differences are attributable to the strong dependence in the transition states on the total angular momentum. The rate constants obtained from both methods appear to have a strong negative temperature dependence which is in agreement with experiment. The pronounced negative temperature dependence can be ascribed to the results of the coupling between tight dissociation transition states and the loose entrance channel. It can be readily seen from Figure 3 that the *E*,*J*-resolved rate constants can better reproduce experimental values in the temperature range of 300−3000 K.

The calculated rate constants for the total and the two-product channels can be expressed, in units of cm^3 mol^{-1} s^{-1}, by the following equations evaluated for the temperature range 300−3000 K:

$$k_t = 2.80 \times 10^{20}\, T^{-2.39} \exp(-856.7/T)$$

$$k_a = 3.98 \times 10^{19} T^{-2.19} \exp(-877.2/T)$$

$$k_b = 1.46 \times 10^{21}\, T^{-2.74} \exp(-918.0/T)$$

3.3. Product Branching Ratios. Table 4 presents the results for the branching ratio $k_b/(k_a + k_b)$ obtained by *E*-resolved and *E*,*J*-resolved RRKM calculations. The results show that with temperature increasing, the branching ratio, $k_b/(k_a + k_b)$, decreases slowly (see Figure 4). In the temperature range of 300−600 K, the branching ratio for CO_2 production varies within the range of 0.52−0.58, which is in good with the experimental values, 0.56 ± 0.07[9] and 0.65 ± 0.06.[12] The branching ratios obtained from both *E*-resolved and *E*,*J*-resolved calculations are almost the same, suggesting that they are independent of angular momentum. As mentioned previously, at the BAC-MP4 level,[16] the reproduction of the experimentally observed branching ratio[9] by conventional RRKM calculations required a downward adjustment of transition-state energy for channel (a) by 3.6 kcal (15% of the barrier height). At the BAC-MP4 level,[16] the energy difference between TS2 and TS3 is 9.5 kcal/mol; at the G2M level, it is 8.2 kcal/mol. Therefore, the better branching ratio predicted by G2M was due in part to the difference in the energies between the two transition states and in part to the difference in ZPEs (or vibrational frequencies) predicted by the two methods. Obviously, the G2M method is more reliable for prediction of both transition-state energies and for their vibrational frequencies at least for the present system.

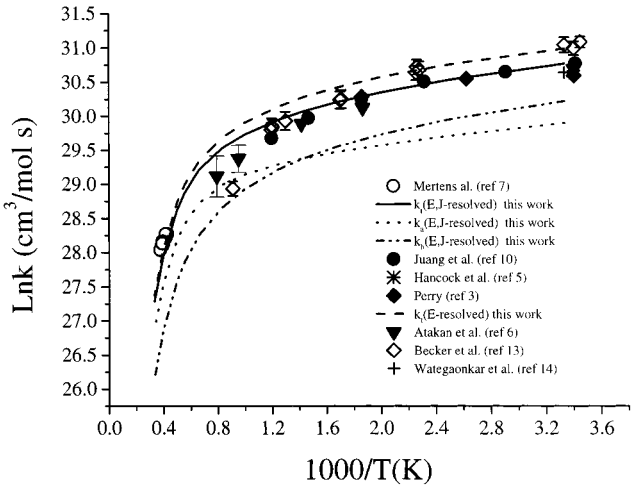

Figure 3. Comparison of the experimental and calculated rate constants.

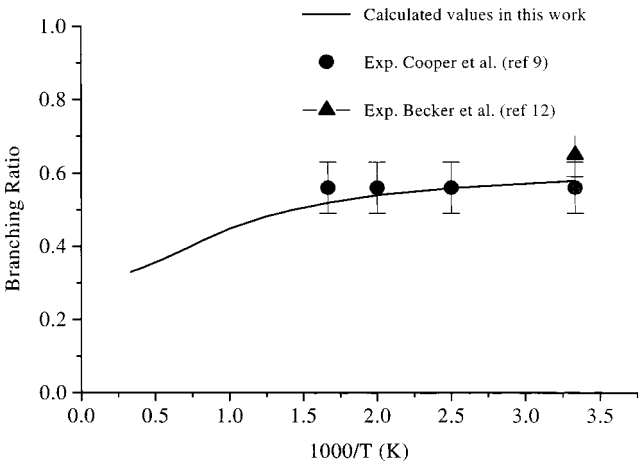

Figure 4. Branching ratio for the production of N_2 and CO_2 via channel (b) as a function of temperature.

Concluding Remarks

The strong negative temperature dependence of the experimental results for the total and individual rate constants could be reproduced and explained by microcanonical *E*,*J*-resolved variational RRKM calculations based on the energies and molecular parameters predicted by the G2M method. With the temperature increasing, the enhanced redissociation of inter-

mediate cis-OCNNO back to the reactants results in the observed strong negative temperature dependence as was concluded by our previous calculations.[16]

The branching ratio $k_b/(k_a + k_b)$ decreases slowly with temperature, the predicted value is in good agreement with the experimental results in temperature range 300−600 K. The good agreement in the total rate constant and the branching ratio between theory and experiment suggests the reliability of the G2M method for energy prediction and the versatility of the variable, flexible transition-state approach for barrierless reactions.[30,31]

Acknowledgment. This work was sponsored partially by Emory University and partially by the Caltech MURI project under ONR Grant No. N00014-95-1388, Program Manager Dr. J. Goldwasser. We thank Professors S. J. Klippenstein and D. M. Wardlaw for helpful discussions on the use of the Variflex program and also thank the Cherry L. Emerson Center for Scientific Computation for the use of computational programs and CPU time.

References and Notes

(1) Perry, R. A.; Siebers, D. L. *Nature* **1986**, *324*, 657.
(2) Miller, J. A.; Bowman, C. T. *Int. J. Chem. Kinet*. **1991**, *23*, 289.
(3) Perry, R. A. *J. Chem. Phys.* **1985**, *82*, 5485.
(4) Cookson, J. L.; Hancock, G.; Mckendrick, K. G. *Ber. Bunsen-Ges. Phys. Chem*. **1985**, *335*, 89.
(5) Hancock, G.; Mckendrick, K. G. *Chem. Phys. Lett*. **1986**, *127*, 125.
(6) Atakan, B.; Wolfrum, J. *Chem. Phys. Phys. Lett*. **1991**, *178*, 157.
(7) Mertens, J. D.; Dean, A. J.; Hanson, R. K.; Bowman, C. T. *24th Symposium (International) on Combustion*; Combustion Institute: Pittsburgh, 1992; p 701.
(8) Cooper, W. F.; Hershberger, J. F. *J. Phys. Chem.* **1992**, *96*, 771.
(9) Cooper, W. F.; Park, J.; Hershberger, J. F. *J. Phys. Chem*. **1993**, *97*, 3283.
(10) Juang, D. Y.; Lee, J. S.; Wang, N. S. *Int. J. Chem. Kinet.* **1995**, *27*, 111.
(11) Brownsword, R. A.; Hancock, G. *J. Chem. Soc. Faraday Trans.* **1997**, *93*, 2473.
(12) Becker, K. H.; Kurtenbach, R.; Wiesen, P. *Chem. Phys. Lett.* **1992**, *198*, 424.
(13) Becker, K. H.; Kurtenbach, R.; Schmidt, F.; Wiesen, P. *Ber. Bunsen-Ges. Phys. Chem.* **1997**, *101*, 128.
(14) Wategaonkar, S.; Setser, D. W. *J. Phys. Chem*. **1993**, *97*, 10028.
(15) Jones, W. E.; Wang, L. *Can. J. Appl. Spectrosc*. **1993**, *38*, 32.
(16) Lin, M. C.; He, Y.; Melius, C. F. *J. Phys. Chem*. **1993**, *97*, 36.
(17) Melius, C. F.; Binkley, J. S. *20th Symposium (International) on Combustion*; Combustion Institute: Pittsburgh, 1984; p 575.
(18) Melius, C. F. In *Chemistry and Physics of Energetic Materials*; Bulusu, S., Ed.; NATO ASI 309, 1990; p 21.
(19) Ho, P.; Melius, C. F. *J. Phys. Chem.* **1990**, *94*, 5120.
(20) Forst, W. *Theory of Unimolecular Reactions*; Academic Press: New York, 1973.
(21) Becke, A. D. *J. Chem. Phys*. **1993**, *98*, 5648.
(22) Becke, A. D. *J. Chem. Phys*. **1992**, *96*, 2155.
(23) Becke, A. D. *J. Chem. Phys*. **1992**, *97*, 9173.
(24) Lee, C.; Yang, W.; Parr, R. G. *Phys. Rev*. **1988**, *B37*, 785.
(25) Gonzalez, C.; Schlegel, H. B. *J. Phys. Chem*. **1989**, *90*, 2154.
(26) Mebel, A. M.; Morokuma, K.; Lin, M. C. *J. Chem. Phys*. **1995**, *103*, 7414.
(27) Frisch, M. J.; Trucks, G. W.; Schlegel, H. B.; Gill, P. M. W.; Johnson, B. G.; Robb, M. A.; Cheeseman, J. R.; Keith, T.; Petersson, G. A.; Montgomery, J. A.; Raghavachari, K.; Al-Laham, M. A.; Zakrzewski, V. G.; Ortiz, J. V.; Foresman, J. B.; Cioslowski, J.; Stefanov, B. B.; Nanayakkara, A.; Challacombe, M.; Peng, C. Y.; Ayala, P. Y.; Chen, W.; Wong, M. W.; Andres, J. L.; Replogle, E. S.; Gomperts, R.; Martin, R. L.; Fox, D. J.; Binkley, J. S.; Defrees, D. J.; Baker, J.; Stewart, J. P.; Head-Gordon, M.; Gonzalez, C.; Pople, J. A. *GAUSSIAN 98, REVISION A*.1; Gaussian, Inc.: Pittsburgh, PA, 1998.
(28) MOLPRO is a package of ab initio programs written by Werner, H.-J.; Knowles, P. J., with contributions from Almlöf, J.; Amos, R. D.; Berning, A.; Cooper, D. L.; Deegan, M. J. O.; Dobbyn, A. J.; Eckert, F.; Elbert, S. T.; Hampel, C.; Lindh, R.; Lloyd, A. W.; Meyer, W.; Nicklass, A.; Peterson, K.; Pitzer, R.; Stone, A. J.; Taylor, P. R.; Mura, M. E.; Pulay, P.; Schütz, M.; Stoll; H.; Thorsteinsson, T.
(29) Chakraborty, D.; Park, J.; Lin, M. C. *Chem. Phys*. **1998**, *231*, 39.
(30) Klippenstein, S. J. *Chem. Phys. Lett*. **1990**, *170*, 71; *J. Chem. Phys.* **1991**, *94*, 6469; *J. Chem. Phys*. **1992**, *96*, 367.
(31) Robertson, S. H.; Wagner, A. F.; Wardlaw, D. M. *J. Chem. Phys*. **1995**, *103*, 2917.
(32) Gilbert, R. G.; Smith, S. C. *Theory of Unimolecular Reactions*; Blackwell, Cambridge, MA, 1990.
(33) Klippenstein, S. J.; Wagner, A. F.; Dunbar, R. C.; Wardlaw, D. M.; Robertson, S. H. *VARIFLEX: VERSION 1.00*, **1999**.
(34) Aubanel, E. E.; Wardlaw, D. M. *J. Phys. Chem*. **1989**, *93*, 3117.
(35) Wardlaw, D. M.; Marcus, R. A. *J. Phys. Chem*. **1986**, *90*, 5383.